Effect of Potassium on the Mechanisms of Biomass Pyrolysis Studied using Complementary Analytical Techniques

Yann Le brech, Thierry Ghislain, Sébastien Leclerc, Mohammed Bouroukba, Luc Delmotte, Nicolas Brosse, Colin Snape, Patrick Chaimbault, Anthony Dufour

Effect of potassium on the mechanisms of biomass pyrolysis as studied by in-situ ^{1}H NMR, TG-DSC and LC/MS

Yann Le Brech[1], Thierry Ghislain[1], Sebastien Leclerc[2], Mohamed Bouroukba[1], Luc Delmotte[3], Nicolas Brosse[4], Colin Snape[5], Anthony Dufour[1]

[1] LRGP, CNRS, Université de Lorraine, 1 rue Grandville 54000 Nancy, France

[2] LEMTA, CNRS, Université de Lorraine, BP 54506 Vandoeuvre lès Nancy

[3] IS2M, CNRS, Université de Haute Alsace, 15 rue Jean Starcky BP 2488 68057 Mulhouse cedex, France

[4] LERMAB, Université de Lorraine, BP239 54506 Vandoeuvre lès Nancy cedex, France

[5] Faculty of Engineering, , The University of Nottingham, Energy Technologies Building, Nottingham NG2 2 TU, United Kingdom

Abstract

Complementary analytical methods have been usedto study the effect of potassium on the primary pyrolysis mechanisms of cellulose and miscanthus. Thermogravimetry, calorimetry, high temperature ^{1}H NMR (in-situ and real time analysis of the fluid phase formed during pyrolysis) and water extraction of quenched char followed by SEC/MS-ELSD (size exclusion chromatography coupled with mass spectrometry and evaporative light scattering detector have been combined). Pyrolysis was conducted under fixed bed conditions to impose similar mass transfer conditions as TGA/DSC and^{1}H NMR to produce charfor SEC/MS. Potassium impregnated in cellulose suppresses the formation of anhydro-sugars measuredby SEC/MS, reduces the formation of mobile protons as observed by in-situ ^{1}H NMR and gives rise to a mainly exothermic signal (by calorimetry). Interestingly, the evolution of mobile protons formed from K-impregnated cellulose follows with a very similar pattern the evolution of the mass loss rate with the mobile protons are formed before mass loss commences during pure cellulose pyrolysis. This methodology has been also applied to miscanthus, demineralised miscanthus, potassium re-impregnated miscanthus after demineralization, raw oak and douglas fir. We discuss the mechanism of primary pyrolysis of biomass and notably highlight the importance of the intermediate liquid phase.

1 Introduction

Faced with growing concern over the excessive emissions of greenhouse gases lignocellulosic biomass has been recognized as a promising alternative and carbon-neutral renewable source for biofuels and chemicals[1]. Thermo-chemical processes (gasification, pyrolysis, combustion and liquefaction) are serious options in order to transform biomass into energy or materials.[2] All of these transformation technologies involve pyrolysis as the initial transformation step.[3,4] For this reason, the chemical mechanism of biomass pyrolysis have been extensively studied for over a century.[5,6] Lignocellulosic biomass composition varies among biomass species and growing conditions but it consists generally of carbohydrates (~70 wt%), lignin (10-30 wt%), extractibles, and ashes. Inorganic materials come mainly from mineral nutrients necessary for plant growth and life. The mineral content depends on genotype, harvest time, location and also fertilization.[2,7] Basically, minerals represent less than 1 wt% of dry biomass, however the content can reach 15 wt% in some forestry residues or herbaceous biomass.[8,9] The major inorganic elements are silicon, alkali, alkaline earth metallic and transition metals[10], which could have significant catalytic effects on the chemical mechanisms of biomass pyrolysis and for this reason they have been extensively studied.[9,11–17] Furthermore, inorganic constituents significantly modify the pyrolysis products (char, bio-oil and gas) distribution and composition.[15,18,19] Their presence not only leads to catalytic effects but also contributes to several problems in the thermo-chemical processes such as a decrease in the quality of bio-oil, syngas or exhaust gas.[8,20]

In order to investigate the influence of inorganic consitutents during biomass pyrolysis removal[8,9,14,19,21–24] and/or impregnation[12,19,25] of biomass with mineral matters have been studied by various treatments.

The most convenientmethod to remove inorganic materials from biomass is eaching with water or acids.[9] Treatments with strong acids (hydrochloric, sulfuric or nitric) are the most efficient techniques for removing inorganics but it could alter the biomass structure[8,9,26] and therefore it could be an important artifact leading to an incorrect conclusion about the effect of inorganic materials. On the other side water leaching and hydrofluoric acid treatment do not affect significantly the structure of biomass[9,27] albeit these treatments are not as efficient as strong acid ones concerning inorganic removal. Regards water leaching, previous investigations showed that this method is selective for potassium (K) and sodium (Na) removal.[8,9,14,28]

Potassium has an important catalytic role on the chemical mechanisms of biomass pyrolysis and it has been extensively investigated.[22,27,29,30] Based on previous thermo-gravimetric analysis (TGA) of different biomasses (Table 1), the main influences according to potassium are: 1) it lowers the initial temperature decomposition; 2) increases the char yield; 3) lowers the maximum degradation rate; 4) lowers the temperature for maximum degradation. Studies have also been conducted on individual biomass components indicating that potassium has a similar impact on cellulose.[12,22] These studies show that the influence on the hemicelluloses (xylan) is not so important[12,22]. TGA results about K-impregnated lignins show inconsistent results, however it is known that potassium could promotes several chemical reactions such as demethoxylation, demethylation, condensation and Cγ-elimination during lignin pyrolysis.[17,31,32]

Potassium not only controls product distributiosn but it also significantly impacts the composition of the products. Pyrolysis combined with Gas Chromatography (Py-GC)[15,32], GC/Mass Spectrometry (MS)[27], TG-MS[18,33], on-line MS[34,35], TGA-FTIR[22,36,37] have been used in order to investigate the effect of potassium on

the composition of volatiles. Nuclear Magnetic Resonance (NMR) has been also used for char analysis.[38] All theses investigations confirm that K-impregnation of cellulose or biomass has the following effect on pyrolysis: 1) it increases char and gas yield at the expense of bio-oils; 2) higher yields in lower molecular weight species (aldehydes and acid light compounds) and lower yields in levoglucosan are produced. During pyrolysis, potassium increases the formation of this lower molecular weight species by fragmentation, ring opening and dehydration[37] reactions and inhibits the formation of anhydrosugars.[35,39]

Table 1. Initial temperature decomposition (Ti), maximum degradation rate temperature (Tmax) and char weight yield (%char) for different biomass samples and various potassium contents

	Raw			K-doped			Water leached			heating rate	ref
Sample	Ti	Tmax	%char	Ti	Tmax	%char	Ti	Tmax	%char	°C/min	
Wheat straw	225	342	22% (700°C)					397	12,3% (700°C)	10	22
Yellow poplar wood		356	6,8% (800°C)					374	4,4% (800°C)	10	27
Willow, 1wt%K ($KC_2H_3O_2$)		374	12,3% (900°C)		313	19,8% (900°C)				25	36
Miscanthus Giganteus	200	355	28,1% (900°C)				250	365	18,6% (900°C)	10	26
Poplar wood	220	362	14,9% (700°C)				220	376	11,4% (700°C)	10	9
Wheat straw	200	320	75,3% (300°C)				200	354	79,9% (300°C)	5	40
Miscanthus Sinensis			22% (900°C)						14,5% (900°C)	20	18
Cellulose cotton 1wt%K (K_2CO_3)	263	372	9% (600°C)	185	357	21,6% (600°C)				20	37
Cellulose, 1wt%K ($KC_2H_3O_2$)		368	7,7% (900°C)		325	27,7% (900°C)				25	12

During biomass pyrolysis, the formation of a liquid intermediate phase has been observed.[41–44] This intermediate is very important for chemical mechanisms occurring during pyrolysis because it is a precursor of gas/volatiles/char and it can strongly control the composition of products. The composition of the liquid intermediate phase produced during cellulose fast pyrolysis has been analysed by Lédé et al.[45] and Piskorz et al.[46] A recent work[47] provides an experimental evidence and quantification of this intermediate liquid-phase by *in-situ* ^{1}H NMR (or Proton magnetic resonance thermal analysis PMRTA[48]) during biomass pyrolysis.

H transfer from H donor' intermediate products to H acceptors are important pyrolysis mechanisms[34,49,50]. For this reason, the analysis of mobile protons by *in situ* ^{1}H NMR investigation is an interesting method to better understand the mechanism of pyrolysis. This investigation shows that the presence of inorganic materials can reduce mobility development during biomass pyrolysis by the inhibition of cellulose

depolymerization.[47] However, this study has been conducted on biomass treated by a strong acid inducing biomass structural degradation. The liquid intermediate phase during slow pyrolysis of cellulose have been investigated by water extraction and further analysis of water-soluble compounds (by using high-performance anion-exchange chromatography with pulsed amperiometric detection HPAEC-PAD).[51] Similar studies have been performed on cellulose fast pyrolysis with different salt impregnations.[52,53] These experiments have been extensively discussed highlighting interesting effects on cellulose pyrolysis mechanisms. The depolymerization, which occurs during pure cellulose pyrolysis and produces mainly anhydro-sugars, seems to be inhibited in the presence of salts whereas the pyrolysis of impregnated-cellulose leads to a more cross-linked structure.

To the best of our knowledge and despite all these previous studies, the detailed chemical effects of inorganic materials and especially of potassium during pyrolysis are still poorly understood because of the heterogeneity of the various samples and conditions tested. The most advanced kinetic mechanisms does not yet take into account the role of inorganic materials[54]. Therefore, there is still a strong need to develop original experimental methods in order to better understand the effect of inorganic materials during pyrolysis.

The aim of this study is to provide a multi-analytical investigation combining TGA, Differential Scanning Calorimetry (DSC), *in-situ* ^{1}H NMR, Size Exclusion Chromatography (SEC)-MS in order to get a better understanding of the effect of potassium during biomass pyrolysis. It is important that these analyses are conducted under controlled mass and heat transfer conditions. This study focuses on well characterized biomasses (Miscanthus x Giganteus, Douglas fir and Oak) and on pure commercial cellulose. The influence of potassium during the fluid phase development is highlighted by our in-situ analysis. It confirms that minerals directly interact with the biomass structure and generate specific primary chemical pathways.

2 Material and methods

2.1 Characterization of biomass samples

Miscanthus x Giganteus was harvested in Lorraine (France) in 2011. Douglas and Oak were harvested in the Haut-Beaujolais area (South-East France). They were milled and sieved to a particle size between 40 and 100µm. This particle size was kept constant for all characterizations and pyrolysis experiments.
Samples have been analyzed by ICP-OES and ICP-MS following the CNRS-SARM procedure[55] in order to characterize their mineral and organic matter contents.
Carbohydrates and Klason lignin contents were measured on extractive free material according to the NREL procedure[56] and the analysis was repeated at least three times (standard deviation presented in sup. material). Samples were hydrolyzed by concentrated sulfuric acid (72%) for 1h in a rotary water bath at 30°C and then autoclaved during 1h30 after being diluted to 3% sulfuric acid through addition of water. The autoclaved sample were filtered, and then dried to give the Klason lignin content. Monosaccharides in the filtrate were quantified using high-performance anion-exchange chromatography with pulsed amperiometric detection (HPAEC-PAD). Microgranular cellulose was purchased from Sigma Aldrich (ref. C6413).

2.2 Demineralization and impregnation procedures

Biomass (10 g) was washed two times by ultra-pure water at 90°C for 2 hours.[9] The remaining inorganic materials were quantified by ICP-OES and ICP-MS following CNRS-SARM procedure.[55]
Biomass, demineralized biomass and cellulose were impregnated by the incipient wetness method with potassium acetate to yield of 1 wt% of potassium based on dry biomass. 3 g of dry biomass were contacted with 1.27 mL of a potassium acetate solution in deionized water (0,06 g/ml). Biomass was carefully stirred to ensure a good distribution of potassium. Then, the sample was dried at 80°C for a night.

2.3 Thermogravimetric and differential scanning calorimetry analysis

Samples were analysed by thermo-gravimetric analysis using Mettler Toledo (Stare System) apparatus. These analyses were conducted on 5 mg of each sample, put into a graphite crucible, heated at 5 K/min up to 500°C. The carrier gas was purified Argon at 100 Nml/min. Differential scanning calorimetry analysis were performed on a SETARAM DSC 111 calorimeter equipped by an original fixed bed set up (Figure 1) in order to better control mass transfer during analysis. Approximately 30 mg of each sample was heated at 5 K/min up to 500°C. The sample was flushed by purified argon gas at 20 Nml/min.[57]

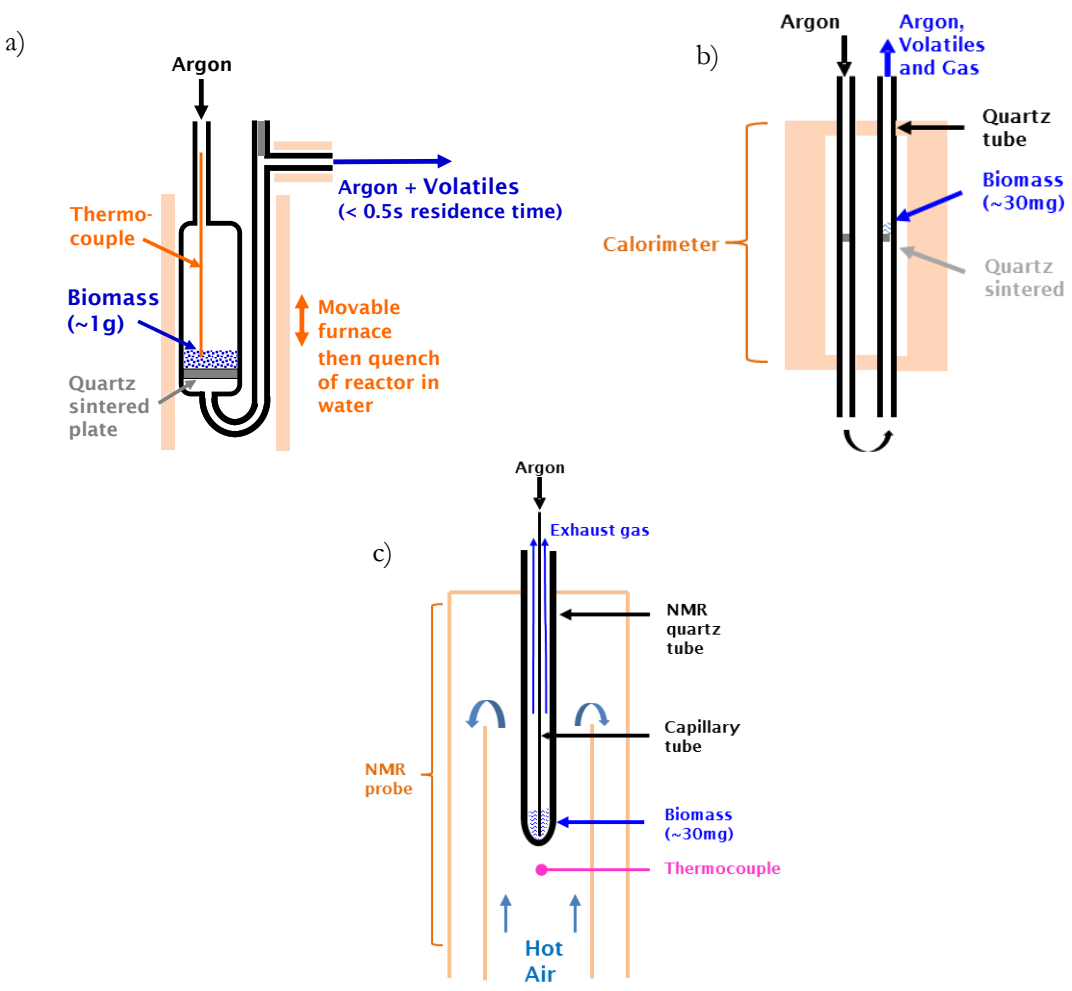

Figure 1. Simplified scheme of a) U-shape quartz fixed bed, b) calorimeter fixed bed, c) ^{1}H NMR High temperature probe equipped with flushing gas

The carrier gas velocity was kept constant between the 3 devices to get similar mass transfers within the fixed beds of particles.

2.4 Pyrolysis experiments in fixed bed reactor

A larger mass of biomass (800 mg) was pyrolysed in a vertical U-shape quartz fixed bed reactor (Figure 1) in order to extract from the char (quenched at various final temperatures) a sufficient amount of intermediate species for further analysis. Biomass particles were supported on quartz sintered plate (20 mm internal diameter). This geometry allows a good control of temperature, thanks to a thermocouple (0.5 mm diameter) inside the fixed bed of biomass particles, and of mass transfer by flushing the fixed bed with a given flow rate of Argon (300 NmL/min). The reactor was heated by an electrical furnace from 20°C to targeted temperature at a heating rate of 5 K/min. The gradient inside sample was estimated to 10°C between the middle and the outer surface of the bed. Once the set temperature was achieved, the furnace was immediately moved down and the reactor was immediately immersed in ice-water in order to quench the char by a rapid cooling (maximum 2 minutes cooling from 500°C to 150°C). Char was cooled down under Argon until 30°C and then collected for further analysis such as water extraction and LC/MS analysis (see section 2.6.).

2.5 *In-situ* ^{1}H NMR analysis

A Bruker 200 MHz NMR instrument was used in conjunction with a high temperature probe equipped by a proprietary device in order to improve mass transfer during pyrolysis inside the probe (Figure 1). Approximately 30 mg of each sample were put inside the NMR quartz tube which was equipped by a thin glass capillary line in order to flush the sample inside the tube with purified argon during pyrolysis, in a similar way than in all the other fixed bed devices (Figure 1). The flow rate was set at 10 Nml/min. A piece of quartz wool was placed on the top of the sample in order to avoid any particles entrainment. A temperature calibration was realized by comparing temperature given by the probe and temperature inside the sample. A thermocouple was put inside the sample during a blank test and temperature was increased to 500°C under inert atmosphere. Then the temperature correction factor has been established. As already described in previous investigation[47], the spectra were deconvoluted using a Matlab program into Gaussian (solid-like) and Lorentzian (liquid-like) distribution functions (see ref. [47] for more details). The amount of fluid phase (% Mobility) is calculated from the following relation:

$$\%H_L = A_L/(A_L+A_G)$$

Where A_L and A_G are the areas of Lorentzian and Gaussian functions respectively.

All the carrier gas flow rates for fixed bed DSC, fixed bed U-shape reactor and *in-situ* ^{1}H NMR tests were set to keep the samecarrier gas velocity in each set-up.

2.6 Characterization of water-soluble fractions from biomass chars

In this study, the solid residue (char) obtained after various final temperature by the fixed bed U-shape reactor was separated into water-soluble and water-insoluble fractions. Approximately 150 mg of the solid residue were immersed in demineralized water (10 ml) at ambient temperature during 30 minutes under stirring. The mixture was filtered to obtain the liquid containing soluble species. Aqueous solutions were analyzed by a total organic carbon analyzer (TOC Shimadzu V_{CSH}) in order to determine the total carbon content in the solution. The yield of water soluble species was calculated on a carbon basis via normalizing the total water-soluble carbon in pyrolyzed cellulose to the total carbon in raw cellulose[51] (Yield %C). Water-soluble fractions were also analyzed by HPLC-SEC-MS/Evaporative Light Scattering Detector (ELSD) Separation was performed on a Shimadzu LC-MS 20 equipped with two SEC PL aquagel-OH 20 columns provided by Agilent. Mobile phase was composed of methanol/water 50:50 v/v, ammonium acetate (100 μM) and formic acid (0.1 %) were added to improve electrospray ionization. The flow rate was maintained at 0.4 mL/min, resulting pressure in the columns was 50 bar, oven temperature was set at 40°C. A split was placed after the separation and a flow of roughly 10 μL/min were sent to the mass spectrometer and the rest was diverted to the ELSD. Mass spectrometry settings were set as followed: interface voltage – 4.5 kV, interface temperature: 350 °C, heat block temperature: 150°C, nitrogen nebulization gas: 1.5 L/min, nitrogen drying gas: 3 L/min. Data from the Shimadzu ELSD were acquired at 10 Hz rate and temperature was set at 40°C.

3 Results and discussion

3.1 Characterization of biomass

The inorganic metal contents for all the samples are presented in Table 2. Cellulose microgranular (Cel_micro) shows absolutely no detectable inorganic material and Cellulose impregnated by 1 %wt of potassium (Cel_1K) shows a content of 0.9 %wt of potassium. Miscanthus was treated with water as described previously in order to remove inorganic materials (Misc_Demin). The mass loss occurring during this procedure was 5 %wt (on dry biomass basis). This loss could be due to smooth hemicellulose hydrolysis and/or extractible solubilization. In order to estimate the impact of the water treatment on biomass, carbohydrates, the Klason lignin and the inorganic metal contents were compared before and after the water treatment. The comparison of monomeric sugar contents (Table 3) shows that there is no signifcanteffect on the composition of the raw material after the treatment and that the hemicellulosic sugars are well preserved after demineralization as described in the literature.[9] The investigation of the inorganic elemental contents after water treatment indicates that only potassium is removed from the biomass as already described.[14,58]

Table 2. Inorganic elementalcontents in sample before and after mineralization/demineralization

	%wt dry biomass										
	Si	**Al**	**Fe**	**Mn**	**Mg**	**Ca**	**Na**	**K**	**Ti**	**P**	**Total**
Cellulose	0,01	0,00	0,00	0,00	0,00	0,00	0,01	0,00	0,00	0,00	0,00
K-impregnated Cellulose	0,00	0,00	0,00	0,00	0,00	0,00	0,01	0,90	0,00	0,00	0,92
Miscanthus	2,15	0,25	0,13	0,02	0,13	0,53	0,02	0,65	0,01	0,01	3,90
Misc_Demin	1,80	0,23	0,15	0,02	0,09	0,31	0,02	0,09	0,02	0,01	2,74
Douglas	0,01	0,00	0,00	0,01	0,00	0,03	0,00	0,02	0,00	0,00	0,08
Oak	0,03	0,01	0,01	0,01	0,01	0,14	0,00	0,11	0,00	0,01	0,34

Table 3. Compositions before and after demineralization

	%wt biomass (extractible free)							
Samples	**Klason lignin**	**Organic matter**	**Total Sugars**	**Arabinose**	**Galactose**	**Glucose**	**Xylose**	**Mannose**
Miscanthus	29,8	92,4	70,2	2,3	0,6	48,9	18,3	0,0
Misc_Demin	28,3	94,8	71,7	2,9	0,7	46,6	20,9	0,0

3.2 Effect of carrier gas velocity on the pyrolysis regimes

In order to reduce secondary reactions and to study primary mechanisms, the flow rate of carrier gas has been optimized for all fixed bed devices. The residence time is one of the most important parameters according to pyrolysis operations. For this reason, the influence of the flow rate have been investigated by DSC[57] and also by ^{1}H-NMR analysis. DSC analysis showed that there is no significant effect of flow rate (from 20 NmL/min) when a fixed bed is used. These results are confirmed by *in-situ* ^{1}H-NMR investigations. Figure 2 shows that the presence of carrier gas has an important effect on the fluidity development during miscanthus pyrolysis. Without carrier gas, the fluidity remains at higher temperatures because the carrier gas improves the devolatilisation of the intermediate liquid-phase. Mass transfer effects are very well known in pyrolysis[59,60] and is here demonstrated by our *in-situ* analysis. Different flow rates of carrier gas were studied up to 15 Nml/min. The effect of the gas flow is weak between 5 and 15 Nml/min (Figure 2). Consequently under these conditions the pyrolysis is conducted close to chemical regime conditions.

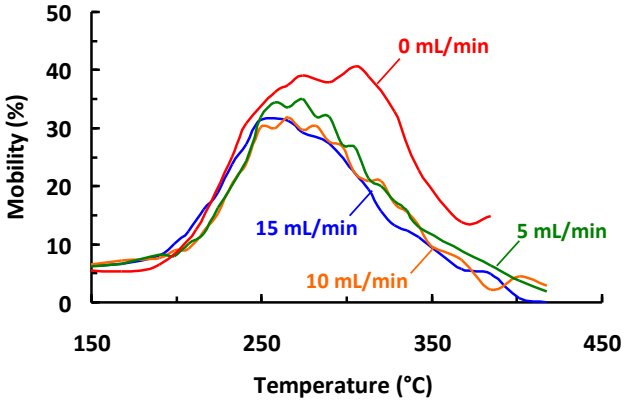

Figure 2. Effect of carrier gas flow rate on fluidity development during Miscanthus pyrolysis

The char yield is a good indicator of the heat and mass transfer conditions occurring during pyrolysis. The char yields obtained from the four devices are comparable (Table 4) except for the ^{1}H NMR probe. In the latter case, the char yield is higher because the maximum temperature was limited to 420°C to protect the probe. Experiments with 800 mg sample mass (in the U-shape fixed bed reactor) gave the same char yield than experiments with 5 mg in the TGA. Char yields are very near for all methods at 500°C final temperature demonstrating that these experiments were conducted under similar mass and heat transfer conditions and thus very close to the pure chemical regime.

Table 4. Comparison of char yields for the different experimental techniques (*NMR at 420°C final temperature)

	%wt dry biomass at 500°C			
Samples	**Fixed bed**	**DSC**	**^{1}H in situ NMR***	**TG**
Miscanthus	29	29	32	29
Misc_Demin	-	16	21	16
Cellulose	7	7	13	7
K-impregnated cellulose	-	21	28	26
Douglas	21	19	26	20
Oak	19	18	27	19

3.3 Effect of potassium on cellulose pyrolysis

In order to have a better understanding of the influence of potassium (K) during cellulose pyrolysis, the thermal behavior of cellulose microgranular and 1 %K-impregnated cellulose have been investigated by TGA, DSC and *in situ* ^{1}H NMR. Chars produced by the fixed bed pyrolysis at selected temperatures were submitted to aqueous extractions to identify and quantify the water-soluble pyrolysis products. Figure 3 presents the differential thermo-gravimetric (DTG) signal (% wt/s), the DSC results (mW/mg), the amount of fluid ^{1}H (% mobility) and the yield of water soluble species (yield % C, as analyzed by TOC) as a function of pyrolysis final temperature.

The comparison between the pure and the impregnated cellulose DTG signals indicates theimportant effect of the potassium during pyrolysis. These results are in close agreement with literature data[12,37]. Cellulose exhibits a degradation curve with one main peak which reaches a maximum decomposition rate at 330°C whereas impregnated cellulose shows a DTG curve with two peaks, at a maximum mass loss rate at 213°C and 320°C, respectively. Char yields from TGA, DSC and ^{1}H NMR analysis (Table 4) are much higher for the K-impregnated cellulose. The comparison between the two DSC analysis profiles (Figure 3) shows that the decomposition of cellulose which is mainly endothermic, becomes slightly exothermic with the addition of 1% wt K without any detectable endothermic peak. The pure cellulose gives an endothermic thermogram, it mostly undergoes depolymerization reactions which induce the formation of anhydro-sugars by transglycosylation.[34] Consequently, the overall reaction is mainly endothermic due to the rupture of glycosidic bonds and to the evaporation of depolymerized products.[59–61] This depolymerization may not involve mass loss because it produces oligomers which have a too high molecular weight to be devolatilised. At higher temperatures the polymerization degree is further reduced and lower molecular weight species (anhydro-sugars, mainly levoglucosan) can devolatilise. Concerning the impregnated cellulose, the first degradation step (213°C) observed in the DTG signal could be due to the production and volatilization of low molecular weight molecules (acids) and gas (CO_2 and CO).[36,37] At higher temperature, the transglycosylation reactions are inhibited by potassium and ring opening, fragmentation and dehydration are favoured[32,35,39]. Ab-initio modeling has shown that the complexation of potassium with cellulose hydroxyl and ether groups may stabilize a particular conformation of the glycosidic bond and therefore promote ring opening and cracking of glycosidic linkage[24]. Crosslinking reactions are promoted by potassium leading to a higher char yield and to an exothermic signa overalll[59,62]. The exothermic signal is also promoted by the formation of a higher yield in aromatic structures[38].

The inhibition of the transglycosylation, which leads to levoglucosan formation, has been highlighted recently by activation energies based on MBMS experiments[35]. The addition of potassium also induces a significant impact on fluidity development (Figure 3). The fluidity development of cellulose starts at 250°C and reaches its maximum at 300°C (20% of mobile H) and decreases to5% at 400°C. The development occurs before any mass loss illustrating the formation of a "fluid phase cellulose" as already observed and discussed in our previous investigation[47], which corresponds to the formation of an intermediate material extensively studied[5] and identified by several names (active cellulose[63], intermediate carbohydrates[38], depolymerized cellulose[64]). This active cellulose undergoes further depolymerization to generate a pool of intermediate species (levoglucosan, cellobiosan, etc.)[45,46] until the devolatilisation of the lighter ones. Conversel,y the fluidity development of impregnated cellulose exhibits a very similar pattern compared to the mass loss probably because the small molecules formed by the fragmentation reactions give rise to a fluid phase which is easily devolatilised. Fwewermobile protons entrapped in the char are produced for the impregnated cellulose (Figure 3). The decrease in mobile protons by K-catalyzed pyrolysis could arise due to the enhancement of homolytic scission imposed by potassium due to the conformation of pyranose ring in the presence of potassium[65]. Furthermore the mobile protons may stabilise the free radicals formed during pyrolysis[50]. In other words, the enhanced formation of radicals could reduce the number of mobile ^{1}H protons.

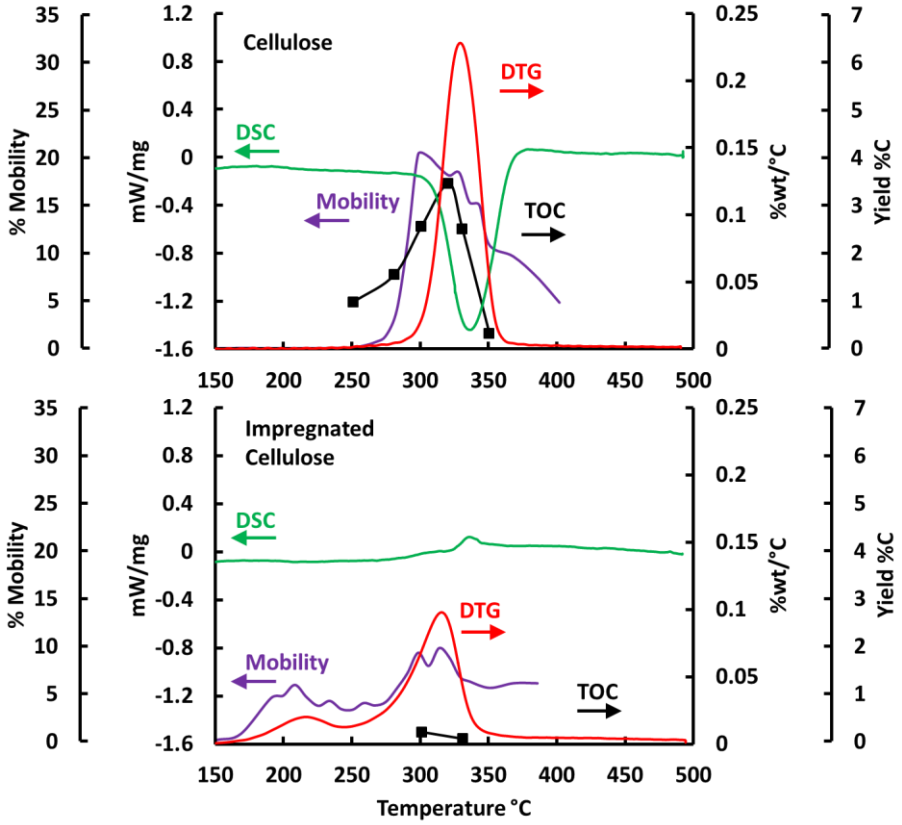

Figure 3. DSC, DTG , % Mobility and TOC evolution as function of temperature for Cellulose and Impregnated Cellulose

Chars produced at different temperatures with the U-shape fixed bed reactor have been separated into water-soluble and water-insoluble fractions. The water soluble fractions have been analyzed by SEC-MS/ELSD and the ELSD chromatograms are presented in Figure 4. The water-soluble levoglucosan and cellobiosan contents have been quantified atdifferent temperatures and the yields obtained are presented in Figure 5. One can notice a similar pattern for levoglucocan and cellobiosan formation (Figure 5), both beingformed after the formation of an intermediate liquid phase (as analysed by in-situ ^{1}H NMR) composed of depolymerized cellulose, confirming previous findings[43,46,51]. The formation of this intermediate liquid phase does depend on the crystallinity and degree of polymerisation of the cellulose.[51,66,67] Concerning the water-soluble fractions from the pure cellulose chars, only anhydro-sugars (DP 1-5) have been identified by mass spectrometry (see supplementary material for themass spectra and major ions formed).. No sugars (cellobiose, etc.) have been detected confirming that transglycosylation is the main chemical pathway occurring during pyrolysis of pure cellulose. Concerning K-impregnated cellulose, TOC values are much lower than for pure cellulose (Figure 3). The liquid intermediate species are devolatilised quickly and poorly retained in the char. The char structure is more “cross linked” due to the impact of potassium, also explaining the poor water solubility.[53] Furthermore, no anhydro-sugar has been detected in the water-soluble fraction from the impregnated cellulose char, confirming that transglycosylation is no longer occurringduring pyrolysis. For all the samples, a peak is observed at a retention time of 34.5 minutes (Figure 4). This peak seems to be more important for the impregnated cellulose. Unfortunately the MS analysis did not allow us to make any qualitative investigation about this peak (too high molecular weight). This peak could correspond to a high molecular weight intermediatewhich is water-soluble and composed of cross-linked glucose units.

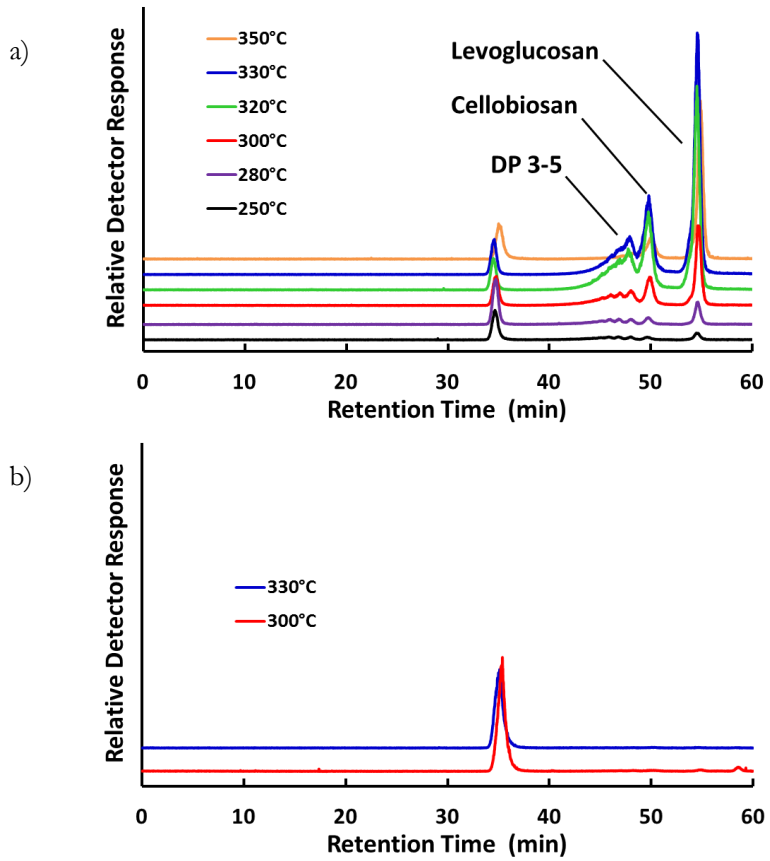

Figure 4. Effect of pyrolysis temperature on the composition of water soluble compounds extracted from char quenched at various pyrolysis temperatures for a) cellulose and b) K-impregnated cellulose

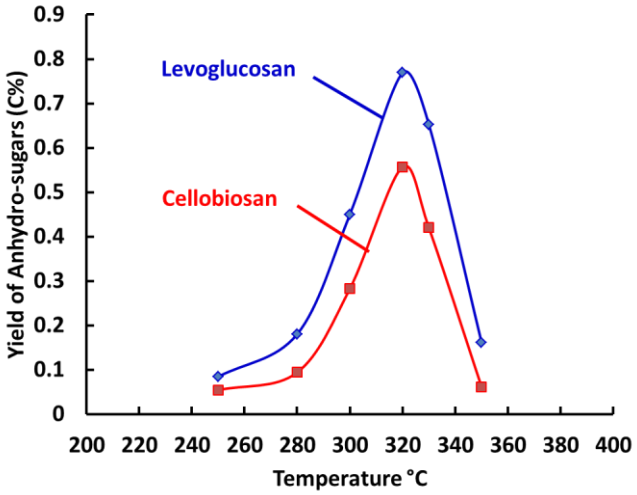

Figure 5. Quantification of the levoglucosan and cellobiosan in the water soluble fractions extracted from char quenched at various pyrolysis temperatures for pure cellulose

3.4 Effect of demineralization and potassium impregnation on Miscanthus pyrolysis

Figure 6 presents the DTG curve (%wt/s), DSC signal (mW/mg), amount of fluid ^{1}H (% mobility) and the yield of water soluble species (Yield %C) as function of temperature for miscanthus, demineralized miscanthus (Misc_Demin) and demineralized miscanthus followed by an impregnation with 1 %wt. of potassium (Misc_Demin_1K). The miscanthus mass loss starts at 200°C and reaches a maximum at 320°C. The DSC profile exhibits a first exothermic peak and a second endothermic which give roughly a thermoneutral signal (compared to pure cellulose signals). Miscanthus is composed of hemicelluloses, lignin, cellulose and minerals involving various chemical reactions with a balance between endo- and exothermic reactions. The fluidity analyzed by in-situ ^{1}H NMR starts to increase quickly at 200°C and reaches a maximum at 270°C.

Concerning demineralized miscanthus (Misc_Demin), the mass loss starts at 220°C with a shoulder (295°C) more pronounced than for raw miscanthus and followed by a maximum at 340°C (320°C for raw miscanthus). The maximum mass loss rate (0.117 %wt/s) is higher than for raw miscanthus (0.068 %wt/s). These results are in close agreement with previous investigations.[9,26,28] The shoulder at 295°C could be attributed to hemicellulose degradations and the peak at 340°C to cellulose degradation. The shoulder is more pronounced after the demineralization because demineralization does not affect significantly the DTG signal for xylan and lignin but it increases the maximum mass loss rate of cellulose and shifts the maximum degradation to higher temperature. The fluidity starts to increase at 200°C and reaches a maximum at 270°C as already observed for miscanthus. The maximum value of the fluid phase is similar (around 30 %mobile H) for Misc_Demin and miscanthus but the fluidity remains stable for Misc_Demin until 350°C whereas it decreases for raw miscanthus from 300°C. The higher content in potassium in raw char leads to an important decrease of fluidity development from cellulose pyrolysis (as discussed in section 2.3). This observation is supported by the DSC investigation. The pyrolysis of demineralised miscanthus is mainly endothermic due to the removal of inorganic materials which promote crosslinking reactions. However the analysis of water-soluble compounds by HPLC (Figure 7) does not reveal any anhydro-sugars formed during the pyrolysis of demineralised miscanthus unlike pure cellulose. Indeed it remains inorganic materials into biomass even after demineralization which could still inhibit transglycosylation reactions of cellulose.

When 1% wt K is added to the demineralized miscanthus, the behaviour becomes similar to those obtained for the raw miscanthus (Figure 6). The DTG profile shows one peak degradation step which reaches a maximum at 320°C and the DSC thermogram is very similar to the raw miscanthus one. However the % mobility profile is slightly different. The demineralization step has removed other inorganic materials than potassium (Ca, Mg, etc, see table 2) and the impregnation by potassium (after =demineralization) may involve different forms and locations of the potassium in the macromolecular network compared to the raw miscanthus. Although the maximum fluidity is different for the two samples, the shape of the mobility curve is similar. Indeed, the maximum fluidity and the decrease in fluidity development occur at the same temperatures (270 and 300°C respectively (Figure 6). When potassium is added, it modifies the degradation of cellulose as already discussed (Section 2.3). The addition of potassium reduces the maximum fluidity (at 270°C) which is mainly developed in this temperature zone by hemicelluloses conversion[47].

What about TOC analysis? No significant effect because still minerals remaining extracted on hemicelluloses zone ? maybe cellulose zone at 340°C ?

Similarly to cellulose, a peak is observed by HPLC for the water soluble fractions in all cases at the retention time of 34.5 minutes. Although any investigation by MS were not possible, the evolution of the absolute intensity/area is in agreement with previous results (Section 2.3). The signal for this high moelcular weight speciesincreases with the presence of potassium in the sample.

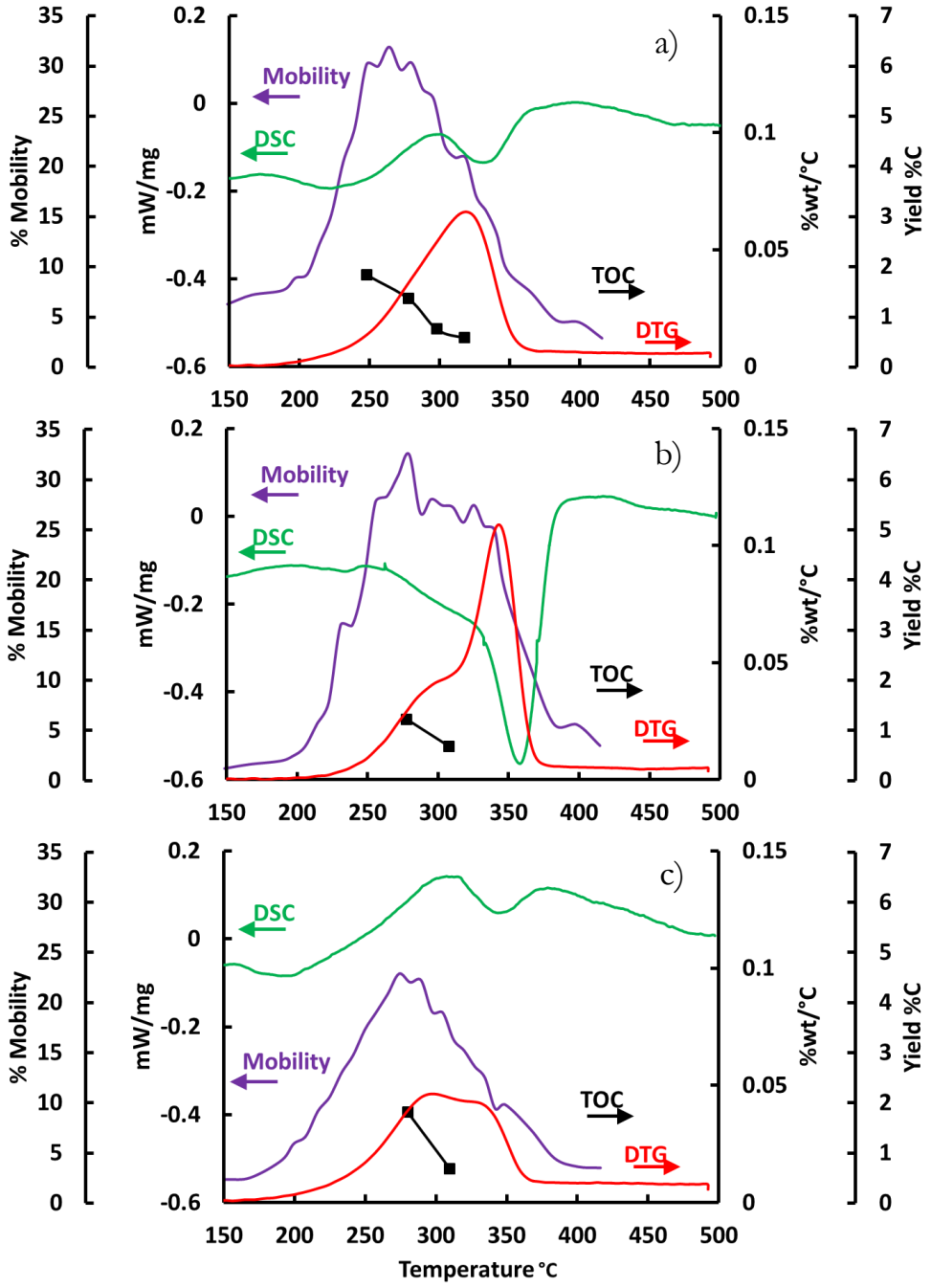

Figure 6. DSC, DTG, ^{1}H NMR and TOC for a) Miscanthus, b) Misc_Demin, c) Misc_Demin_1K

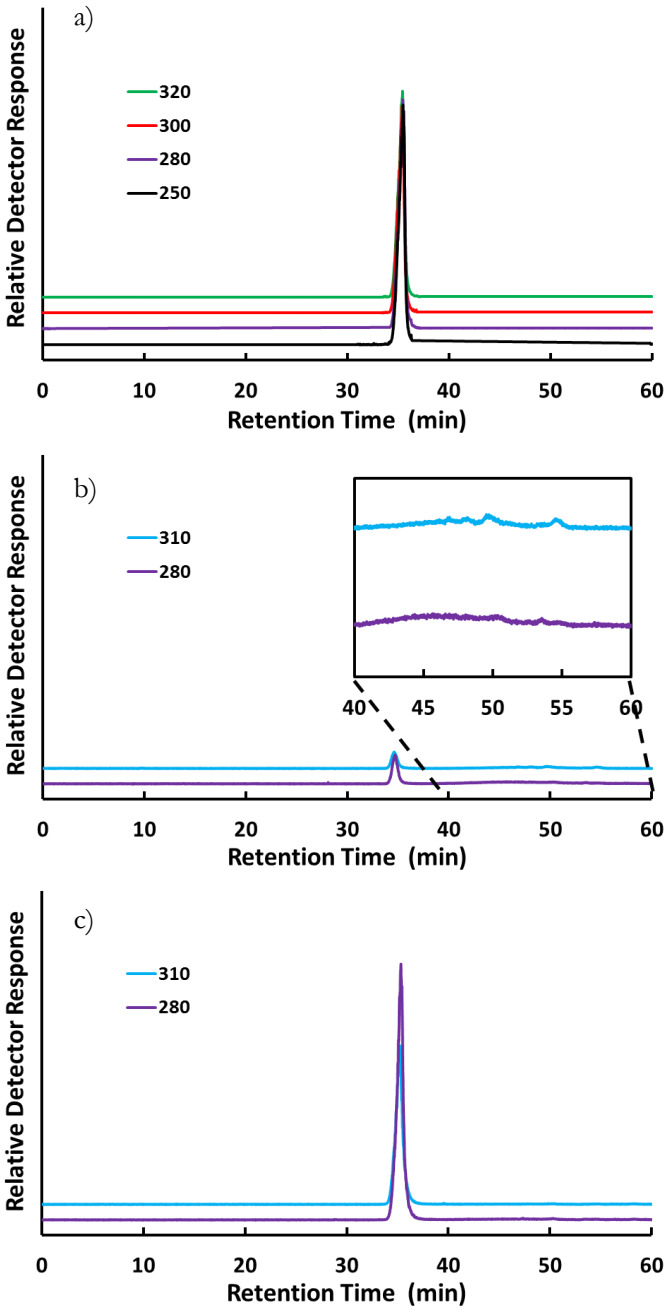

Figure 7. SEC-DEDL of water extracted Misc. a), water Misc_Demin b), water Mis_Demin_1K c)

3.5 Pyrolysis behaviour of douglas fir and oak

The same multi-analysis approach has been used on oak and douglas fir (Figure 8). Oak and douglas exhibit a global endothermic behavior whereas miscanthus is both slightly exothermic and then endothermic. A weak exothermic peak can also be detected for oak pyrolysis at about 300°C. These differences could be mainly attributed mainly to the different amounts of inorganicspecies present. Douglas fir and oak contain much lower concentrations of inorganic elementsthan miscanthus (Table 2). The higher concentrations in miscanthus (especially K, Ca, Mg, Fe) promotes cross-linking (exothermic) reactions. DTG curves of douglas and oak present a shoulder at 280°C and 310°C for oak and douglas respectively, which is attributed to hemicelluloses conversion. This difference can mainly be explained by the different compositions of the

hemicelluloses. Douglas hemicelluloses are composed predominantly by glucomannan (C6 pyranose) whereas oak hemicelluloses are composed by xylan (C5 pyranose), therefore it induces different thermal stabilities.[68] Xylan is less stable than mannan exhibiting a more pronounced shoulder for oak pyrolysis. The peak of maximum mass loss rate (340 and 350°C for oak and douglas, respectively) is attributed to cellulose decomposition. Oak has a higher inorganic content (notably Ca^{2+} and K^{+}). It is known that ash content of coniferous trees is usually smaller than deciduous trees and coniferous wood often decomposes at higher temperature ranges in TG experiments.[28]

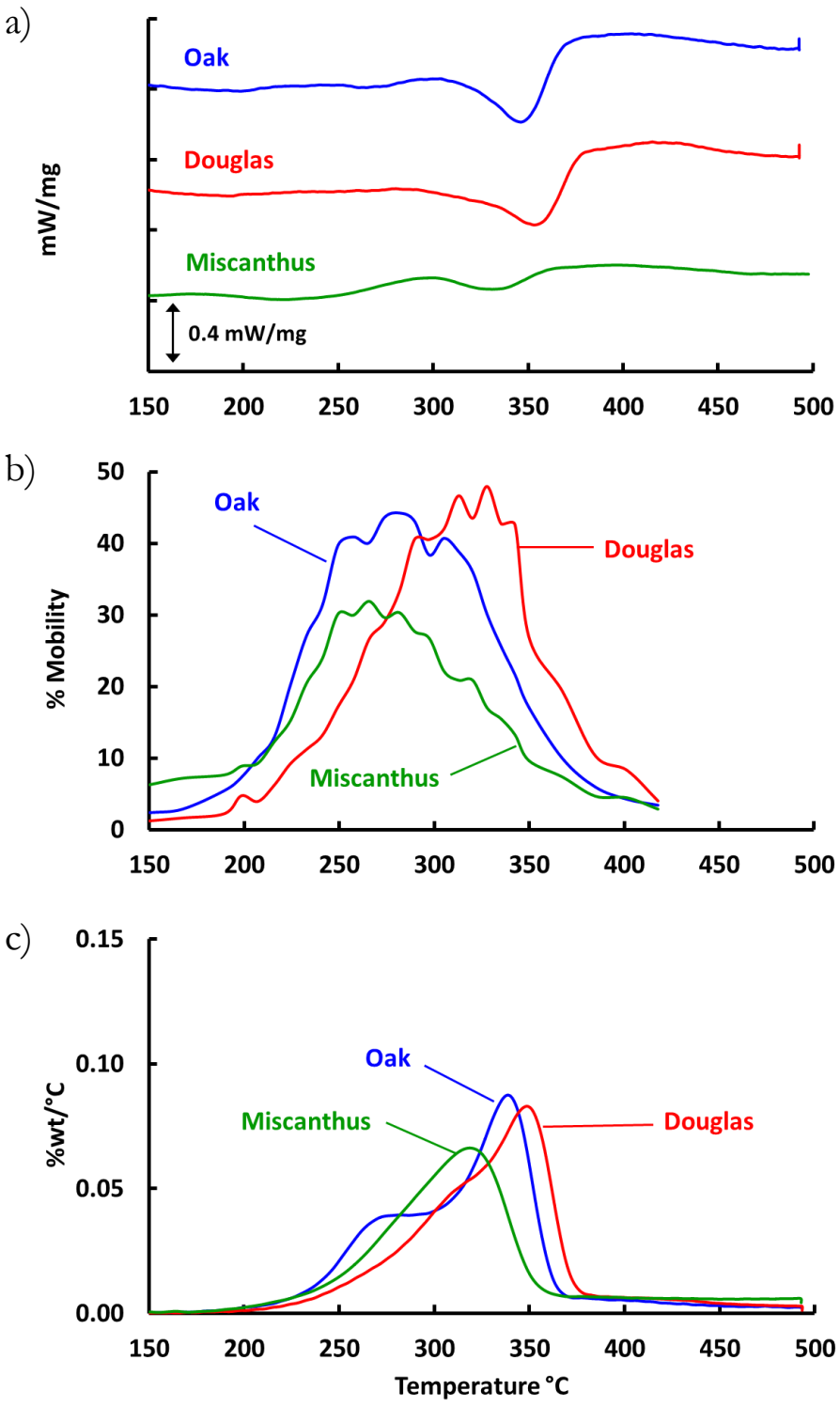

Figure 8. Miscanthus, douglas, oak : a) DSC, b) ^{1}H NMR c) DTG

Inorganic element and hemicelluloses contents also impact are the fluidity developments (Figure 8). The mobility development starts at 200°C (from lignin conversion[47]) for the three biomasses but the maximum fluidity occurs at higher temperature for douglas than for oak and miscanthus.

4 Conclusion

As far as we know, this work presents for the first time the combination of: (1) TG-DSC, (2) in-situ ^{1}H NMR analysis of mobile protons, (3) water extraction of chars followed SEC/MS-ELSD to analyse the intermediate species during primary pyrolysis of biomass. The complementary analytical methods are conducted under similar mass transfer effects very close to the pure chemical regime. They are used to better understand the impact of potassium on the pyrolysis mechanism of cellulose and of ligno-cellulosic biomass (miscanthus). This methodology is applied to other biomasses (oak and douglas fir) with different content in inorganic materials and different composition in the macromolecules (mainly hemicelluloses). Potassium impregnated in cellulose suppresses the formation of anhydro-sugars, reduce the formation of mobile protons and give rise to a mainly exothermic signal whereas the pyrolysis of pure cellulose gives an endothermic signal. Interestingly, the pyrolysis characteristics of a raw and demineralized miscanthus followed by re-impregnation with potassium are similar and the evolution of mobile protons formed during K-impregnated cellulose follows with a very similar pattern the evolution of the mass loss rate while the mobile protons are formed before the mass loss for pure cellulose pyrolysis. The *in situ* ^{1}H NMR analysis appears to be an original analytical tool in order to better understand the importance of the intermediate "liquid" phase formed during biomass pyrolysis.

Acknowlegments

The authors gratefully acknowledge the financial support of the French research national thorough the project "PYRAIM" (ANR-11BS09-003) and of the CNRS interdisciplinary program thorough the project "FORêVER". F. Mathieu (LRGP-CNRS) is acknowledged for some help on the Matlab program used for deconvolution of ^{1}H NMR spectra. S. Pontvianne (LRGP-CNRS) is acknowledged for the optimization of the total organic carbons method and for some help on the SEC/MS-ELSD method.

Supplementary materials

Data provided in the supplementary material:

- detailed analysis of sugar and inorganic contents of the biomasses,
- detailed procedure for in-situ ^{1}H NMR analysis
- reproducibility of the ^{1}H NMR fixed bed probe,
- mass spectra and ionisation mechanisms by Electro Spray Ionisation of water extract from char

References

(1) Ragauskas, A. J.; Williams, C. K.; Davison, B. H.; Britovsek, G.; Cairney, J.; Eckert, C. A.; Frederick, W. J.; Hallett, J. P.; Leak, D. J.; Liotta, C. L.; Mielenz, J. R.; Murphy, R.; Templer, R.; Tschaplinski, T. The Path Forward for Biofuels and Biomaterials. *Science* **2006**, *311* (5760), 484–489.

(2) Brosse, N.; Dufour, A.; Meng, X.; Sun, Q.; Ragauskas, A. Miscanthus: A Fast-Growing Crop for Biofuels and Chemicals Production. *Biofuels Bioprod. Biorefining* **2012**, *6* (5), 580–598.

(3) Mettler, M. S.; Vlachos, D. G.; Dauenhauer, P. J. Top Ten Fundamental Challenges of Biomass Pyrolysis for Biofuels. *Energy Environ. Sci.* **2012**, *5* (7), 7797–7809.

(4) Huber, G. W.; Iborra, S.; Corma, A. Synthesis of Transportation Fuels from Biomass: Chemistry, Catalysts, and Engineering. *Chem. Rev.* **2006**, *106* (9), 4044–4098.

(5) Lédé, J. Cellulose Pyrolysis Kinetics: An Historical Review on the Existence and Role of Intermediate Active Cellulose. *J. Anal. Appl. Pyrolysis* **2012**, No. 0.

(6) Klason, P.; Heidenstam, G. V.; Norlin, E. Investigations on the Charring of Wood. **1910**, *23*, 1252–1257.

(7) Baxter, L. L.; Miles, T. R.; Miles Jr., T. R.; Jenkins, B. M.; Milne, T.; Dayton, D.; Bryers, R. W.; Oden, L. L. The Behavior of Inorganic Material in Biomass-Fired Power Boilers: Field and Laboratory Experiences. *Fuel Process. Technol.* **1998**, *54* (1–3), 47–78.

(8) Jiang, L.; Hu, S.; Sun, L.-S.; Su, S.; Xu, K.; He, L.-M.; Xiang, J. Influence of Different Demineralization Treatments on Physicochemical Structure and Thermal Degradation of Biomass. *Bioresour. Technol.* **2013**, *146*, 254–260.

(9) Eom, I.-Y.; Kim, K.-H.; Kim, J.-Y.; Lee, S.-M.; Yeo, H.-M.; Choi, I.-G.; Choi, J.-W. Characterization of Primary Thermal Degradation Features of Lignocellulosic Biomass after Removal of Inorganic Metals by Diverse Solvents. *Bioresour. Technol.* **2011**, *102* (3), 3437–3444.

(10) Rutkowski, P. Pyrolysis of Cellulose, Xylan and Lignin with the K2CO3 and ZnCl2 Addition for Bio-Oil Production. *Fuel Process. Technol.* **2011**, *92* (3), 517–522.

(11) Pan, W.-P.; Richards, G. N. Influence of Metal Ions on Volatile Products of Pyrolysis of Wood. *J. Anal. Appl. Pyrolysis* **1989**, *16* (2), 117–126.

(12) Nowakowski, D. J.; Jones, J. M. Uncatalysed and Potassium-Catalysed Pyrolysis of the Cell-Wall Constituents of Biomass and Their Model Compounds. *J. Anal. Appl. Pyrolysis* **2008**, *83* (1), 12–25.

(13) Halpern, Y.; Patai, S. Pyrolytic Reactions of Carbohydrates. VI. Isothermal Decomposition of Cellulose in Vacuo, in the Presence of Additives. *Isr. J. Chem.* **1969**, *7* (5), 685–690.

(14) Fahmi, R.; Bridgwater, A. V.; Darvell, L. I.; Jones, J. M.; Yates, N.; Thain, S.; Donnison, I. S. The Effect of Alkali Metals on Combustion and Pyrolysis of Lolium and Festuca Grasses, Switchgrass and Willow. *Fuel* **2007**, *86* (10-11), 1560–1569.

(15) Patwardhan, P. R.; Satrio, J. A.; Brown, R. C.; Shanks, B. H. Influence of Inorganic Salts on the Primary Pyrolysis Products of Cellulose. *Bioresour. Technol.* **2010**, *101* (12), 4646–4655.

(16) Di Blasi, C.; Galgano, A.; Branca, C. Influences of the Chemical State of Alkaline Compounds and the Nature of Alkali Metal on Wood Pyrolysis. *Ind. Eng. Chem. Res.* **2009**, *48* (7), 3359–3369.

(17) Kleen, M.; Gellerstedt, G. Influence of Inorganic Species on the Formation of Polysaccharide and Lignin Degradation Products in the Analytical Pyrolysis of Pulps. *J. Anal. Appl. Pyrolysis* **1995**, *35* (1), 15–41.

(18) Szabó, P.; Várhegyi, G.; Till, F.; Faix, O. Thermogravimetric/mass Spectrometric Characterization of Two Energy Crops, Arundo Donax and Miscanthus Sinensis. *J. Anal. Appl. Pyrolysis* **1996**, *36* (2), 179–190.

(19) Nik-Azar, M.; Hajaligol, M. R.; Sohrabi, M.; Dabir, B. Mineral Matter Effects in Rapid Pyrolysis of Beech Wood. *Fuel Process. Technol.* **1997**, *51* (1–2), 7–17.

(20) Michel, R.; Kaknics, J.; Bouchetou, M. L.; Gratuze, B.; Balland, M.; Hubert, J.; Poirier, J. Physicochemical Changes in Miscanthus Ash on Agglomeration with Fluidized Bed Material. *Chem. Eng. J.* **2012**, *207–208*, 497–503.

(21) Davidsson, K. O.; Korsgren, J. G.; Pettersson, J. B. C.; Jäglid, U. The Effects of Fuel Washing Techniques on Alkali Release from Biomass. *Fuel* **2002**, *81* (2), 137–142.

(22) Jensen, A.; Dam-Johansen, K.; Wójtowicz, M. A.; Serio, M. A. TG-FTIR Study of the Influence of Potassium Chloride on Wheat Straw Pyrolysis. *Energy Fuels* **1998**, *12* (5), 929–938.

(23) Oudenhoven, S. R. G.; Westerhof, R. J. M.; Aldenkamp, N.; Brilman, D. W. F.; Kersten, S. R. A. Demineralization of Wood Using Wood-Derived Acid: Towards a Selective Pyrolysis Process for Fuel and Chemicals Production. *J. Anal. Appl. Pyrolysis* **2013**, *103*, 112–118.

(24) Saddawi, A.; Jones, J. M.; Williams, A. Influence of Alkali Metals on the Kinetics of the Thermal Decomposition of Biomass. *Fuel Process. Technol.* **2012**, *104*, 189–197.
(25) Zaror, C. A.; Hutchings, I. S.; Pyle, D. L.; Stiles, H. N.; Kandiyoti, R. Secondary Char Formation in the Catalytic Pyrolysis of Biomass. *Fuel* **1985**, *64* (7), 990–994.
(26) Collura, S.; Azambre, B.; Weber, J.-V. Thermal Behaviour of Miscanthus Grasses, an Alternative Biological Fuel. *Environ. Chem. Lett.* **2007**, *5* (1), 49–49.
(27) Hwang, H.; Oh, S.; Cho, T.-S.; Choi, I.-G.; Choi, J. W. Fast Pyrolysis of Potassium Impregnated Poplar Wood and Characterization of Its Influence on the Formation as Well as Properties of Pyrolytic Products. *Bioresour. Technol.* **2013**, *150C*, 359–366.
(28) Müller-Hagedorn, M.; Bockhorn, H.; Krebs, L.; Müller, U. A Comparative Kinetic Study on the Pyrolysis of Three Different Wood Species. *J. Anal. Appl. Pyrolysis* **2003**, *68–69*, 231–249.
(29) Di Blasi, C.; Galgano, A.; Branca, C. Analysis of the Physical and Chemical Mechanisms of Potassium Catalysis in the Decomposition Reactions of Wood. *Ind. Eng. Chem. Res.* **2011**, *50* (7), 3864–3873.
(30) Julien, S.; Chornet, E.; Tiwari, P. K.; Overend, R. P. Vacuum Pyrolysis of Cellulose: Fourier Transform Infrared Characterization of Solid Residues, Product Distribution and Correlations. *J. Anal. Appl. Pyrolysis* **1991**, *19* (0), 81–104.
(31) Sharma, R. K.; Wooten, J. B.; Baliga, V. L.; Lin, X. H.; Chan, W. G.; Hajaligol, M. R. Characterization of Chars from Pyrolysis of Lignin. *Fuel* **2004**, *83* (11-12), 1469–1482.
(32) Eom, I.-Y.; Kim, J.-Y.; Kim, T.-S.; Lee, S.-M.; Choi, D.; Choi, I.-G.; Choi, J.-W. Effect of Essential Inorganic Metals on Primary Thermal Degradation of Lignocellulosic Biomass. *Bioresour. Technol.* **2012**, *104*, 687–694.
(33) Sebestyén, Z.; May, Z.; Réczey, K.; Jakab, E. The Effect of Alkaline Pretreatment on the Thermal Decomposition of Hemp. *J. Therm. Anal. Calorim.* **2010**, *105* (3), 1061–1069.
(34) Evans, R. J.; Milne, T. A. Molecular Characterization of the Pyrolysis of Biomass. 1. Fundamentals. *Energy Fuels* **1987**, *1* (2), 123–137.
(35) Trendewicz, A.; Evans, R.; Dutta, A.; Sykes, R.; Carpenter, D.; Braun, R. Evaluating the Effect of Potassium on Cellulose Pyrolysis Reaction Kinetics. *Biomass Bioenergy* **2015**, *74*, 15–25.
(36) Nowakowski, D. J.; Jones, J. M.; Brydson, R. M. D.; Ross, A. B. Potassium Catalysis in the Pyrolysis Behaviour of Short Rotation Willow Coppice. *Fuel* **2007**, *86* (15), 2389–2402.
(37) Liu, Q.; Wang, S.; Luo, Z.; Cen, K. Catalysis Mechanism Study of Potassium Salts on Cellulose Pyrolysis by Using TGA-FTIR Analysis. *J. Chem. Eng. Jpn.* **2008**, *41* (12), 1133–1142.
(38) Wooten, J. B.; Seeman, J. I.; Hajaligol, M. R. Observation and Characterization of Cellulose Pyrolysis Intermediates by 13C CPMAS NMR. A New Mechanistic Model. *Energy Fuels* **2004**, *18* (1), 1–15.
(39) Piskorz, J.; Radlein, D. S. A. G.; Scott, D. S.; Czernik, S. Pretreatment of Wood and Cellulose for Production of Sugars by Fast Pyrolysis. *J. Anal. Appl. Pyrolysis* **1989**, *16* (2), 127–142.
(40) Saleh, S. B.; Hansen, B. B.; Jensen, P. A.; Dam-Johansen, K. Influence of Biomass Chemical Properties on Torrefaction Characteristics. *Energy Fuels* **2013**, *27* (12), 7541–7548.
(41) Shafizadeh, F.; Fu, Y. L. Pyrolysis of Cellulose. *Carbohydr. Res.* **1973**, *29* (1), 113–122.
(42) Lede, J.; Li, H. Z.; Villermaux, J. Fusion-like Behavior of Biomass Pyrolysis. *Prepr. Pap. - Am. Chem. Soc. Div. Fuel Chem.* **1987**, *32* (2), 59–67.
(43) Boutin, O.; Ferrer, M.; Lede, J. Radiant Flash Pyrolysis of Cellulose -- Evidence for the Formation of Short-Lifetime Intermediate Liquid Species. *J. Anal. Appl. Pyrolysis* **1998**, *47* (1), 13–31.
(44) Axelson, D. E.; Wooten, J. B. Magnetic Resonance Imaging Characterization of Intact Smoked Cigarettes. *J. Anal. Appl. Pyrolysis* **2007**, *78* (1), 214–227.
(45) Lédé, J.; Blanchard, F.; Boutin, O. Radiant Flash Pyrolysis of Cellulose Pellets: Products and Mechanisms Involved in Transient and Steady State Conditions. *Fuel* **2002**, *81* (10), 1269–1279.
(46) Piskorz, J.; Majerski, P.; Radlein, D.; Vladars-Usas, A.; Scott, D. . Flash Pyrolysis of Cellulose for Production of Anhydro-Oligomers. *J. Anal. Appl. Pyrolysis* **2000**, *56* (2), 145–166.
(47) Dufour, A.; Castro-Diaz, M.; Brosse, N.; Bouroukba, M.; Snape, C. The Origin of Molecular Mobility During Biomass Pyrolysis as Revealed by In Situ 1H NMR Spectroscopy. *ChemSusChem* **2012**, *5* (7), 1258–1265.
(48) Mercedes Maroto-Valer, M.; Andrésen, J. M.; Snape, C. E. In Situ 1H NMR Study of the Fluidity Enhancement for a Bituminous Coal by Coal Tar Pitch and a Hydrogen-Donor Liquefaction Residue. *Fuel* **1998**, *77* (9–10), 921–926.
(49) Kotake, T.; Kawamoto, H.; Saka, S. Mechanisms for the Formation of Monomers and Oligomers during the Pyrolysis of a Softwood Lignin. *J. Anal. Appl. Pyrolysis*.
(50) Solomon, P. R.; Hamblen, D. G.; Serio, M. A.; Yu, Z.-Z.; Charpenay, S. A Characterization Method and Model for Predicting Coal Conversion Behaviour. *Fuel* **1993**, *72* (4), 469–488.
(51) Yu, Y.; Liu, D.; Wu, H. Characterization of Water-Soluble Intermediates from Slow Pyrolysis of Cellulose at Low Temperatures. *Energy Fuels* **2012**, *26* (12), 7331–7339.

(52) Liu, D.; Yu, Y.; Long, Y.; Wu, H. Effect of MgCl2 Loading on the Evolution of Reaction Intermediates during Cellulose Fast Pyrolysis at 325 °C. *Proc. Combust. Inst.* **2015**, *35* (2), 2381–2388.
(53) Liu, D.; Yu, Y.; Hayashi, J.; Moghtaderi, B.; Wu, H. Contribution of Dehydration and Depolymerization Reactions during the Fast Pyrolysis of Various Salt-Loaded Celluloses at Low Temperatures. *Fuel* **2014**, *136*, 62–68.
(54) Ranzi, E.; Corbetta, M.; Manenti, F.; Pierucci, S. Kinetic Modeling of the Thermal Degradation and Combustion of Biomass. *Chem. Eng. Sci.* **2014**, *110*, 2–12.
(55) Carignan, J.; Hild, P.; Mevelle, G.; Morel, J.; Yeghicheyan, D. Routine Analyses of Trace Elements in Geological Samples Using Flow Injection and Low Pressure On-Line Liquid Chromatography Coupled to ICP-MS: A Study of Geochemical Reference Materials BR, DR-N, UB-N, AN-G and GH. *Geostand. Newsl.* **2001**, *25* (2-3), 187–198.
(56) Brosse, N.; Sannigrahi, P.; Ragauskas, A. Pretreatment of Miscanthus X Giganteus Using the Ethanol Organosolv Process for Ethanol Production. *Ind. Eng. Chem. Res.* **2009**, *48* (18), 8328–8334.
(57) Lardier, G.; Bouroukba, M.; Le Brech, Y.; Dufour, A. Influence of the Geometry, Particle Sizes and Flow Rate in DSC- In Preparation.
(58) Eom, I.-Y.; Kim, J.-Y.; Lee, S.-M.; Cho, T.-S.; Choi, I.-G.; Choi, J.-W. Study on the Thermal Decomposition Features and Kinetics of Demineralized and Inorganic Metal-Impregnated Lignocellulosic Biomass. *J. Ind. Eng. Chem.* **2012**, *18* (6), 2069–2075.
(59) Mok, W. S.-L.; Antal Jr., M. J. Effects of Pressure on Biomass Pyrolysis. II. Heats of Reaction of Cellulose Pyrolysis. *Thermochim. Acta* **1983**, *68* (2–3), 165–186.
(60) Suuberg, E. M.; Milosavljevic, I.; Oja, V. Two-Regime Global Kinetics of Cellulose Pyrolysis: The Role of Tar Evaporation. *Symp. Int. Combust.* **1996**, *26* (1), 1515–1521.
(61) Arseneau, D. F. Competitive Reactions in the Thermal Decomposition of Cellulose. *Can. J. Chem.* **1971**, *49* (4), 632–638.
(62) Milosavljevic, I.; Oja, V.; Suuberg, E. M. Thermal Effects in Cellulose Pyrolysis: Relationship to Char Formation Processes. *Ind. Eng. Chem. Res.* **1996**, *35* (3), 653–662.
(63) Bradbury, A. G. W.; Sakai, Y.; Shafizadeh, F. Kinetics Model for Pyrolysis of Cellulose. *J Appl Polym Sci* **1979**, *23* (11), 3271–3280.
(64) Mettler, M. S.; Paulsen, A. D.; Vlachos, D. G.; Dauenhauer, P. J. Pyrolytic Conversion of Cellulose to Fuels: Levoglucosan Deoxygenation via Elimination and Cyclization within Molten Biomass. *Energy Environ. Sci.* **2012**, *5* (7), 7864–7868.
(65) Kuzhiyil, N.; Dalluge, D.; Bai, X.; Kim, K. H.; Brown, R. C. Pyrolytic Sugars from Cellulosic Biomass. *ChemSusChem* **2012**, *5* (11), 2228–2236.
(66) Wang, Z.; Pecha, B.; Westerhof, R. J. M.; Kersten, S. R. A.; Li, C.-Z.; McDonald, A. G.; Garcia-Perez, M. Effect of Cellulose Crystallinity on Solid/Liquid Phase Reactions Responsible for the Formation of Carbonaceous Residues during Pyrolysis. *Ind. Eng. Chem. Res.* **2014**, *53* (8), 2940–2955.
(67) Wang, Z.; McDonald, A. G.; Westerhof, R. J. M.; Kersten, S. R. A.; Cuba-Torres, C. M.; Ha, S.; Pecha, B.; Garcia-Perez, M. Effect of Cellulose Crystallinity on the Formation of a Liquid Intermediate and on Product Distribution during Pyrolysis. *J. Anal. Appl. Pyrolysis* **2013**, *100*, 56–66.
(68) Collard, F.-X.; Blin, J. A Review on Pyrolysis of Biomass Constituents: Mechanisms and Composition of the Products Obtained from the Conversion of Cellulose, Hemicelluloses and Lignin. *Renew. Sustain. Energy Rev.* **2014**, *38*, 594–608.